Annals of Anatomy 222 (2019) 12–20

Contents lists available at ScienceDirect

Annals of Anatomy

journal homepage: www.elsevier.com/locate/aanat

RESEARCH ARTICLE

Integrating data on bone modeling and morphological ontogenetic changes of the maxilla in modern humans

Natalia Brachetta-Aporta [a,*], Paula N. Gonzalez [a,b], Valeria Bernal [a,*]

[a] División Antropología, Facultad de Ciencias Naturales y Museo, Universidad Nacional de La Plata, CONICET, La Plata,1900, Argentina
[b] ENyS. Estudios en Neurociencias y Sistemas Complejos, CONICET-HEC-UNAJ., Buenos Aires, Argentina

ARTICLE INFO

Article history:
Received 26 July 2018
Received in revised form 15 October 2018
Accepted 19 October 2018

Keywords:
Facial growth
Histology
Geometric morphometrics
Partial least squares

ABSTRACT

The aim of this work is to assess the association between the patterns of bone modeling and the changes in shape and size of the maxilla along ontogeny in modern humans. The sample analyzed includes an ontogenetic series of 30 individuals from an archeological site from Pampa Grande, northwest of Argentina. The areas of bone resorption and formation were described by histological analysis of bone surfaces and then quantified using spatial statistics. Morphological changes were analyzed by geometric morphometric methods using landmarks and semilandmarks digitized on 3D surfaces obtained from CT-scans. The regression of bone modeling maps on the centroid size shows no significant association between both variables neither in subadult nor adult individuals. On the contrary, the results of the partial least squares analysis shows a strong association between the shape changes in the maxilla with changes in the pattern of bone modeling in both groups of age, subadults and adults. Overall, this study contributes to the understanding of the mechanisms and processes that model maxillary morphology during growth.

1. Introduction

The variation in shape and size of the anatomical structures originates during ontogeny of organisms as a result of processes operating at lower scales of hierarchical organization (eg. cellular, tissular; Atchley and Hall, 1991; Bastir, 2008; Franz-Odendaal, 2011; Hall, 2003; Hallgrimsson and Lieberman, 2008). In particular, bone components are formed during embryonic development by the integration of cellular aggregates whose relative size is controlled by the initial number, the spatial arrangement and the rate of division of the cells, among others. After ossification, the size and shape of these components are regulated by the spatial and temporal changes in the activity of the cells –i.e. osteoblasts and osteoclasts-involved in the processes of bone formation and resorption and passive movements produced by displacement of adjacent tissues (Enlow and Hans, 1996; Frost, 1987; Maggiano, 2012; McCollum, 2008).

The interest in the ontogenetic processes that underlie craniofacial variation in current and extinct populations and species has been renewed in recent years, although most studies focus either on anatomical or histological data. On the one hand, the role of changes in the extension and direction of ontogenetic trajectories has been evaluated by analyzing the shape and size of anatomical structures through geometric morphometric techniques (Gonzalez et al., 2011; Klingenberg, 2016; Mitteroecker and Bookstein, 2008). On the other hand, the study of distribution and extension of the areas of bone formation and resorption has been used to establish the directions of bone growth (Lacruz et al., 2013, 2015a; Martinez-Maza et al., 2013, 2016). However, understanding the growth processes comprehensively requires the integration of both scales to assess how and to what extent the patterns observed at the anatomical scale are a reflection of the processes of bone modeling that occur on a lower scale. Such integration has been hindered, to a large extent, by the disparate methodological approaches employed in the analysis of the two types of data. While morphological analyses have a strong emphasis on the registration of quantitative variables and the use of statistical methods, the histological analysis of bone surfaces has been, until now, descriptive and qualitative (Brachetta-Aporta et al., 2014, 2016; Freidline et al., 2017; Martinez-Maza et al., 2016; Martínez-Vargas et al., 2017; O'Higgins and Jones, 1998). The few studies that analyze the facial morphology and bone modeling patterns on the same samples have been limited to descriptive evaluations of the correspondence between both types of data, standing out for the absence of methods that allow to combine the information in joint statistical analyses.

The objective of the present work is to analyze the bone modeling patterns of the maxilla and the morphological changes along ontogeny in modern humans. In particular, we assess the association between the extent and distribution of the areas of bone

* Corresponding authors.
E-mail addresses: nbrachetta@fcnym.unlp.edu.ar (N. Brachetta-Aporta), bernalv@fcnym.unlp.edu.ar (V. Bernal).

https://doi.org/10.1016/j.aanat.2018.10.008
0940-9602/

formation and resorption with the variation in the shape and size of the maxillary bone. The maxillary bone is of great interest in evolutionary, developmental and biomedical studies (McCollum and Ward, 1997; von Arx and Lozanoff, 2017). It is a complex structure in which skeletal, dental and muscular elements involved in the functions of processing and swallowing food, breathing and speech are integrated (Lieberman, 2011; Moss and Young, 1960). Given its functional relevance and good preservation in the fossil record, the postnatal bone modeling of the maxilla has received special attention, with a focus on the analysis of modern human (Enlow and Bang, 1965; Kurihara et al., 1980; Martinez-Maza et al., 2013; McCollum, 2001, 2008), nonhuman primates (Martinez-Maza et al., 2016; O'Higgins and Jones, 1998; O'Higgins et al., 1991; Wealthall, 2002), and early hominids (Bromage, 1989; Lacruz et al., 2013, 2015a, 2015b).

Here, we analyze an osteological sample of adults and subadults belonging to a prehistoric population from Northwest Argentina. A novel methodological approach is applied to jointly analyze: (a) changes in the morphology of the maxilla during ontogeny using three-dimensional images of computed tomography and geometric morphometric techniques; and (b) the spatial distribution and extension of the areas of bone formation and resorption on bone surfaces by the application of spatial statistics techniques. Finally, the relationship between the morphological changes and the areas of formation and resorption was evaluated by means of partial least squares that allows to identify the variables that underlie the association between the shape of the maxilla and bone modeling processes.

2. Materials and methods

2.1. Samples

We studied the maxillary bone of 30 individuals from archeological samples from Pampa Grande (PG; province of Salta, Northwestern Argentina). This sample was dated to 1720 ± 50 years BP from material associated with bone remains and it has been assigned to Candelaria culture corresponding to the Early Formative period (1500 and 1400 years BP; Baldini et al., 2003; González, 1972; Lema, 2009). The sample belongs to the osteological collections of the División Antropología of Museo de La Plata (Buenos Aires, Argentina).

Previous bioarcheological studies show that PG skulls are characterized by small size and graceful traits (Barbeito-Andrés et al., 2011; Bernal et al., 2006; Gonzalez et al., 2010; Menéndez et al., 2014), and high frequency of tabular cranial deformation (Cocilovo and Varela, 2010). Studies of ancient DNA indicate that individuals from Pampa Grande present a greater diversity than surrounding populations, and are characterized by high frequency of B and D haplogroups (Carnese et al., 2010; Dejean et al., 2014).

According to archeobotanical and faunal remains associated with skeletons, the subsistence of this populations was based on a high diversity of domesticated and wild plants (e.g. *Phaseolus vulgaris, Zea mays, Prosopis* sp., *Cucurbita maxima* sp.), suggesting a horticultural strategy (Baffi et al., 1996; Lema, 2011). Furthermore, the remains found suggest the consumption of wild and domesticated camelids, rodents and, in minor proportion, dasypodidae and fish (V. Lema, pers. comm.).

The dataset comprises CT images from the skulls. CT-scans were obtained in a multi slice scanner of two diagnosis imaging centers from La Plata (CIMED and Mon). The images have a resolution of 1024 × 1024 (voxel size: 0.165 × 0.165 × 0.33 mm) and 512 × 512 (voxel size: 0.345 × 0.345 × 0.33 mm).

Table 1
Composition of the sample.

Group and age range	Features	Total
Subadults		
G1: include up to 4.4 year-old	M1 developed, not PM2 present	4
G2: from 4.5 to 10.4 year-old	M1 eruption, M2 and PM2 developed	8
G3: from 10.5 to 14.4 year-old	M2 and PM2 eruption, M3 developed	2
Adults		
G4: young adult (20–34 year-old)		8
G5: middle-aged adult (35–49 year-old)		8

2.2. Age and sex estimations

Estimations of age and sex of the individuals were made on the basis of morphological traits of craniofacial structures and CT images. Estimations of age were based on dental development and eruption in subadults subjects (AlQahtani et al., 2010; Buikstra and Ubelaker, 1994) and on the degree of obliteration of the sphenobasilar suture and the ectocranial sutures from the latero-anterior region in adults (Buikstra and Ubelaker, 1994; Meindl and Lovejoy, 1985). Subadults were classified in age categories according to the development and eruption of the molars and second premolar. Adults were grouped in the categories proposed by Buikstra and Ubelaker (1994) (Table 1). Additionally, a dental score was obtained for subadults. This score describes the degree of dental development estimated by a Principal Component Analysis (PCA) of the variables that describe the dental formation state of permanent teeth in the maxilla (Brachetta-Aporta, 2018). Deciduous teeth were excluded from the analysis since most of them were lost post-mortem or replaced by permanent teeth. Each tooth was scored with a value between 1 and 14 according to its formation stage, starting from initial cusp formation to apex closure (Buikstra and Ubelaker, 1994). Sex of adults was estimated using the glabella, supraorbital margin, mastoid process, supramastoid crest and nuchal crest (Buikstra and Ubelaker, 1994).

The sample was composed by 14 subadults and 16 adults of both sexes (Table 1). Adults are represented by 11 females and 5 males.

2.3. Morphometric analysis

2.3.1. Shape and size

The morphological variation of the maxillary bone was quantified by means of geometric morphometric techniques (Fig. 1a,b). A total of 21 landmarks and 66 semilandmarks along maxilla contours and surfaces were digitized (Fig. 1b). Landmarks and curve semilandmarks were digitized manually in Avizo 8.0 in order to guarantee its location, while, the surface semilandmarks were digitized by a semiautomatic protocol (Gunz and Mitteroecker, 2013) implemented in *geomorph* and *Morpho* packages for R (R Core Team, 2014). To estimate the intraobserver error associated with the placement of landmarks and semilandmarks, one of us (NBA) obtained two sets of coordinates in 15 skulls. The results obtained show low levels of error (Brachetta-Aporta, 2018).

The differences between configurations of landmarks and semilandmarks due to position, orientation and scale were removed by means of a Generalized Procrustes Analysis (Rohlf and Slice, 1990). To reduce the effects of the initial arbitrary location, the semilandmarks were slid by thin-plate spline (TPS), minimizing the bending energy between the target and reference configurations (Klingenberg, 2013; Mitteroecker and Gunz, 2009). In particular, semilandmarks digitized on curves were slid along tangents while surface semilandmarks were slid along the tangent plane (Gunz and Mitteroecker, 2013). Shape variables were obtained from the coordinates of landmarks and semilandmarks superimposed and slid.

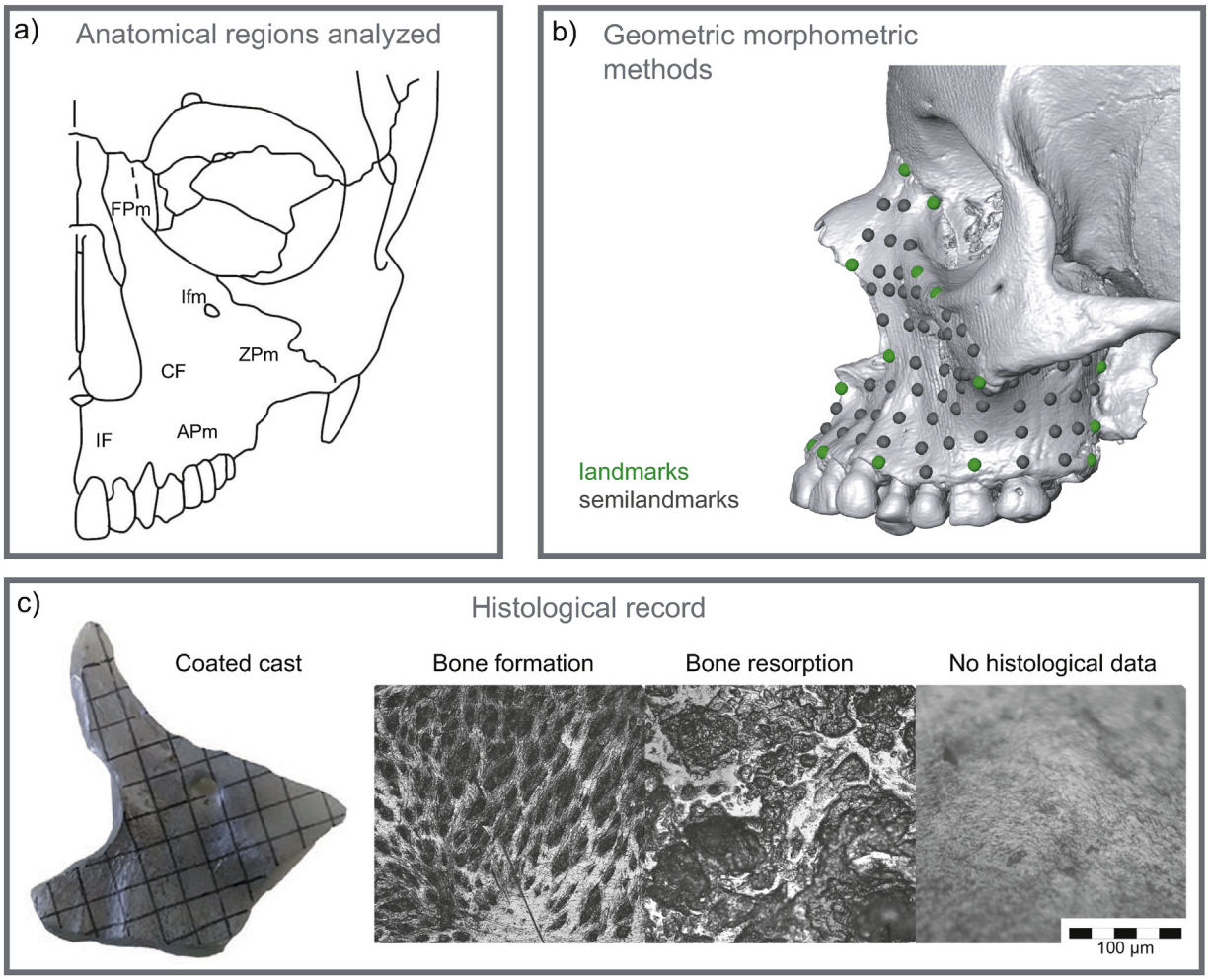

Fig. 1. Summary of the method. (a) Drawing of the left facial skeleton with the regions of the maxilla analyzed: FPm, Frontal Process of maxilla; ZPm, Zygomatic Process of maxilla; APm, Alveolar Process of maxilla; CF, Canine Fossa; IF, Incisive Fossa; Ifm, Infraorbital foramen. (b) Landmarks and semilandmarks digitized on the maxilla. (c) Coated cast with the grid used for observation under the microscope and the bone modeling features identified: mineralized collagen fibers related to bone formation surface, Howship's lacunae related to bone resorption surface, and surfaces with no identified histological features. The grid size is 5 × 5 mm.

The centroid size (CSz; square root of the summed square distance between each landmark and semilandmark to the configuration centroid) was used as a measure of size (Bookstein, 1991).

2.3.2. Analysis of intra-sample morphometric variation

First, shape variation in subadults and adults was analyzed by PCA of the superimposed coordinates. Then, variation in size-related shape changes (i.e. allometric changes) throughout ontogeny was analyzed by a multivariate regression analysis using superimposed coordinates as the dependent variables and the centroid size as the independent variable (Monteiro, 1999). The dependent variable can be read as shape changes per unit of size (or time) increase (i.e. regression score shape; Drake and Klingenberg, 2008). Shape changes with size were represented by morphings (Klingenberg, 2013). The analyses were performed in MorphoJ (Klingenberg, 2011) and R (R Core Team, 2014).

2.4. Histological analysis

2.4.1. Bone surfaces survey

High-resolution casts of the frontal, zygomatic and alveolar processes of the maxilla surface were obtained (Fig. 1a,c). The left side was replicated; however, in cases in which the preservation of the surface prevented the analysis, the right side was replicated. Only individuals with good degree of preservation were included in the sample because taphonomic alterations (e.g. post-deposition bone loss, fragmentation) and/or pathologies (e.g. alveolar resorption due to ante-mortem tooth loss, trauma or abscesses) may alter the fields of bone formation/resorption and modify the normal pattern of bone modeling.

First, the bone surfaces were cleaned using a brush with soft bristles and 60% alcohol. Then, negative casts were made by applying low-viscosity silicon (Coltène® President light body) on the bone surface. These casts were made to produce the positive molds using epoxy resin (Tolken®), which were then covered by a thin layer of gold-palladium (Brachetta-Aporta et al., 2014). This procedure was done at the Museo Argentino de Ciencias Naturales Bernardino Rivadavia. To guide the observation and recording of microstructural bone features under the microscope, a 5 × 5 mm grid was drawn on the positive molds (Fig. 1c).

Two types of bone surfaces were registered based on previous published descriptions (Boyde, 1972; Bromage, 1984; Martinez-Maza, 2007; Martinez-Maza et al., 2010): (a) resorption surfaces that are produced by osteoclast activity and (b) formation surfaces that result from osteoblast activity (Fig. 1c). In brief, bone formation surfaces are characterized by the presence of packs of collagen fibers which are visible as parallel elongated bundles arranged in a predominant direction. Resorption surfaces characteristically present randomly distributed concavities of variable size and shape known as Howship's lacunae. A third type of surface, known as rest-

ing surface, that is associated to the mineralization front, was not included here because of its high similarity to surfaces generated by abrasion as a result of taphonomic processes (e.g. sediment compaction, cleaning, handling; Bromage, 1984) (Fig. 1c). The replicas of bone surfaces were observed using an optical microscope Olympus CX 31 (20× NA 0.40 objective) with incident light. Bone formation and resorption activities were recorded in bone modeling maps, and then scanned and converted to digital images (Brachetta-Aporta et al., 2018). In order to collect better and more accurate data, the intraobserver error associated with the type and extension of the surfaces was previously evaluated by one of us (NBA). This was done by recording the histological data from different casts in three sessions spaced by one week and then comparing the degree of concordance between sessions (Brachetta-Aporta, 2016).

2.4.2. Analysis of intra-sample variation in bone modeling patterns

In order to simultaneously compare several individuals and analyze their variation, bone modeling maps were quantified using the methodology developed in Brachetta-Aporta et al. (2018). Briefly, the procedure involves the construction of consensus configurations of the maxilla maps of the individuals analyzed by a generalized least-squares Procrustes superimposition and thin-plate spline deformation (Bookstein, 1989). The Procrustes superimposition allowed centering, scaling and rotating the maps using the landmarks placed along their contour, so the sum of squared distances between original configurations and the consensus is minimized (Rohlf and Slice, 1990). Then, each rotated image was warped to the consensus configuration – obtained from the superimposition – using thin-plate spline deformation (Bookstein, 1991). These procedures were done in tpsUtil v1.46, tpsDig2 v2.17 and tpsSuper v2.03 (Rohlf, 2015). Because of the differences in maxilla shape and size between subadults and adults, both categories were analyzed separately.

Then, a digital grid was placed on the warped images using ArcGIS 10 (FCNyM licensed). The size of the cells of the digital grid was set to maximize the chances of having only one type of activity (formation or resorption) in each cell (15 × 15 pixels). The information contained in each cell was registered as −1 = presence of bone resorption, 1 = presence of bone formation, 0 = no information available. When more than one type of surface was present in a cell, the most frequent type was registered.

Missing data were estimated using both the information available from the same individual and the information available from the other specimens in the sample. In the first case, a spatial interpolation method was used to estimate the missing values with available information from neighbor cells (Brachetta-Aporta et al., 2018). A semiautomatic protocol developed in ArcGIS 10 was applied to perform the spatial interpolation (Brachetta-Aporta and Gobbo, 2017). A different method was used to estimate areas of missing values for which no data spatially close were present. The procedure developed consists in imputation of missing values using the information from other individuals of the same sample (Brachetta-Aporta, 2018). The estimation was made by *Predictive Mean Matching* (PMM), an algorithm for multiple imputations of missing data when quantitative variables are not normally distributed (van Buuren and Groothuis-Oudshoorn, 2011). The PMM produces imputed values estimating a linear regression with the existing data and then, makes a random draw from the posterior predictive distribution, producing new sets of coefficients for every case (existing and missing) iteratively. This procedure allows determining the relation between existing and estimated data. The analysis was made using the *mice* package for R (R Core Team, 2014).

The information of complete bone modeling maps for each individual was used to perform a PCA to describe the variation in the bone modeling patterns within age groups. Changes in bone modeling patterns were evaluated in relation to the age of the individuals and the maxilla size by means of regression analyses. In order to do so, the PCs which summarize the 80% of variation in subadults and adults were used as dependent variables. The dental score and the centroid size were used as independent variables.

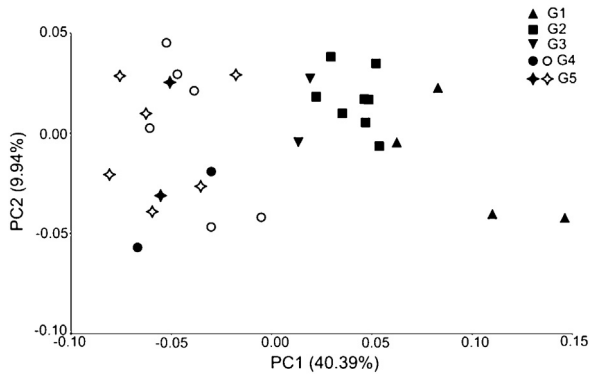

Fig. 2. Principal component analysis of shape coordinates. The PC1 shows a general separation among individuals by age. Subadults: G1, <4.4 years; G2, 4.5–10.4 years; G3, 10.5–14.4 years. Adults: G4, 20–34 years; G5, 35–49 years. Sex of adults is represented as filled (male) and open symbols (female).

On the basis of the individual maps with more than 25% of the total surface with information of bone modeling, a median bone modeling map for each age category was obtained (i.e. subadult and adult). The median value of each cell for both age categories was estimated and then represented in color maps obtained in ArcGIS 10 (Brachetta-Aporta and Gobbo, 2017; Brachetta-Aporta et al., 2018).

2.5. Association between bone modeling patterns and facial morphology

To explore and visualize specific shape changes related to bone modeling, we ran partial least squares (PLS) analyses. The PLS analysis is a linear regression technique that allows to describe the highest mutual covariance between two or more sets, also called blocks, of variables (Abdi, 2010; Bookstein et al., 1990; Rohlf and Corti, 2000). The two sets of variables are treated symmetrically and the resulting coefficients represent the strength of the co-variation between the two blocks (Rohlf and Corti, 2000). This approach is particularly suitable for datasets where a high amount of multicollinearity can be expected (Abdi, 2010). Here, the first block comprises the Procrustes coordinates of maxilla and the second block comprises the principal components that accounted for 80% of variation in bone modeling patterns. The morphometric and statistical analyses were made in Past (Hammer et al., 2001), MorphoJ (Klingenberg, 2011) and R (*geomorph* package; R Core Team, 2014).

3. Results

3.1. Patterns of morphometric variation

The first axis of the principal component analysis performed on the Procrustes coordinates of the maxilla of the adult and subadult individuals summarizes 40.39% of the variation, while the second axis only represents 9.94% of total variation. Subadults and adults are located at opposite extremes of the first principal component (Fig. 2). Accordingly, the regression analysis of Procrustes shape coordinates on the centroid size of the maxilla, which represents the allometric changes within the sample, indicates that 32.82% of the total variation in shape is explained by changes in size (Fig. 3). This regression analysis indicates that the maxilla exhibits an anterior projection and a relatively greater height in larger skulls. The maxillary body shape varies with the increase in size from a

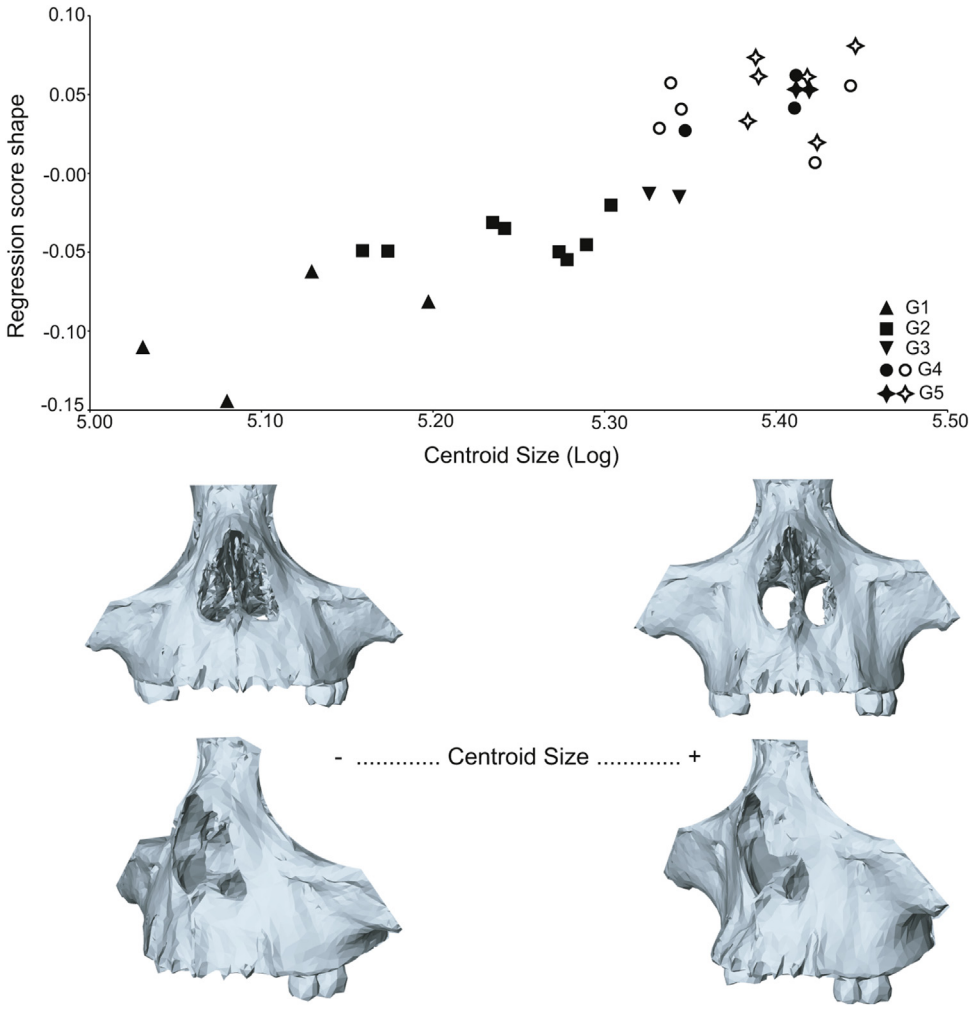

Fig. 3. Regression of the shape variables on centroid size for maxilla of subadults and adults. The morphings represents the variation in shape summarized in the extremes of size. Subadults: G1, <4.4 years; G2, 4.5–10.4 years; G3, 10.5–14.4 years. Adults: G4, 20–34 years; G5, 35–49 years. Sex of adults is represented as filled (male) and open symbols (female).

rounded morphology to a straight body, with an extension of the region between the zygomatic and alveolar processes (Fig. 3).

3.2. Patterns of bone modeling

Fig. 4 shows the PCA of the bone modeling pattern of the subadult (a) and adult (b) maxilla. The first two axes summarize the variation in the distribution of formation and resorption activities. Along the first component, maps are ordered according to the predominant type of surface. In subadults, PC1 summarizes 43.44% of the variation, while in adults, 30.78%. Individuals with predominance of resorption are located in the negative extreme of PC1, while those with larger areas of bone formation are in the positive values. No variation was observed in the pattern of bone modeling associated with the age or sex of the individuals (Fig. 4a,b).

Fig. 5 shows the changes in the pattern of bone modeling associated with age in subadult individuals. In general, the modeling pattern is similar in individuals up to 10.4 years (G1 and G2), but changes in individuals of 10.5–14.4 years (G3). Nevertheless, there is not a clear trend in bone modeling patterns with age.

The general map for the subadult maxilla (Fig. 6a) displays three areas differentiated by the type of predominant bone modeling activity. One of the areas corresponds to the region of the frontal process, characterized by the predominance of bone formation. The second area extends along the canine fossa and the zygomatic process, which displays areas of formation alternated with bone resorption. Finally, the third area corresponds to the alveolar process and is characterized by the predominance of resorption. In adults (Fig. 6b), the three areas delimited in subadults appear as rather continuous areas, maintaining the alveolar process a clearer differentiation. The frontal process presents bone formation, although not in the same extent as in subadults. The regions of the canine fossa and the zygomatic process also have mainly formation, although with some areas of resorption. Some of these areas correspond to those observed in subadults, located above the infraorbital foramen and in the upper part of the zygomatic process. The region of the alveolar process presents bone resorption to a lesser extent than observed for subadults. The region of the incisal fossa presents bone formation. These results indicate that there are changes in the modeling pattern between subadults and adults.

3.3. Association between bone modeling patterns and the morphology of the maxilla

Fig. 7 shows the results of the regression analysis between modeling and centroid size of the maxilla for subadult and adult individuals (a, b respectively). The percentage of variation accounted by size is very low in both groups of age, 11.66% for subadults and 8.07% for adults, which suggests a lack of association between bone modeling and size.

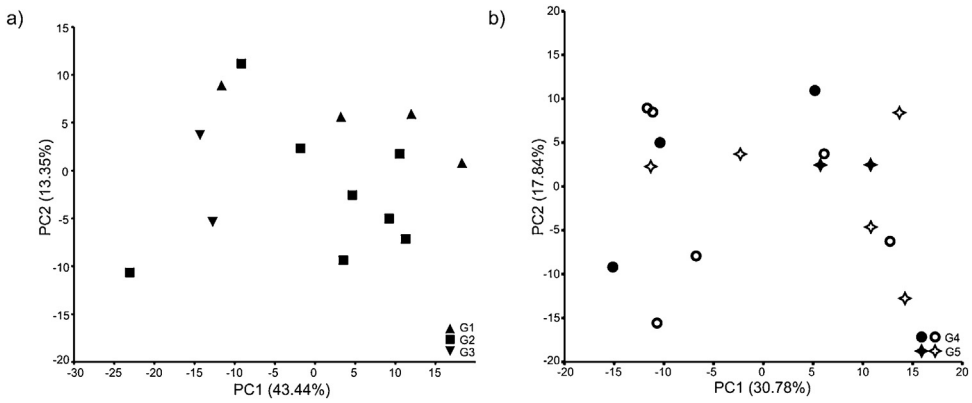

Fig. 4. Principal component analysis of the bone modeling of maxilla in subadults (a) and adults (b). The individuals present a great dispersion across de PC1. Subadults: G1, <4.4 years; G2, 4.5–10.4 years; G3, 10.5–14.4 years. Adults: G4, 20–34 years; G5, 35–49 years. Sex of adults is represented as filled (male) and open symbols (female).

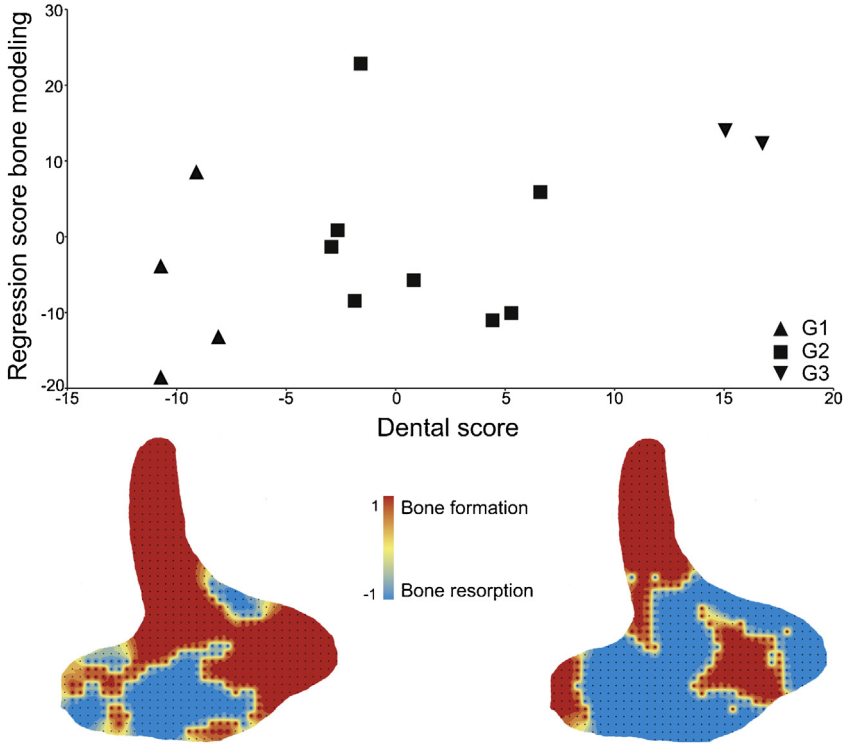

Fig. 5. Regression of bone modeling on age for subadults. Age was obtained from the PC1 of dental development. The variables that summarize the bone modeling pattern correspond to the scores of the PC1 to PC6. The bone modeling maps represent the extremes of the age range; the left is from the youngest subadult and the right from the oldest subadult.

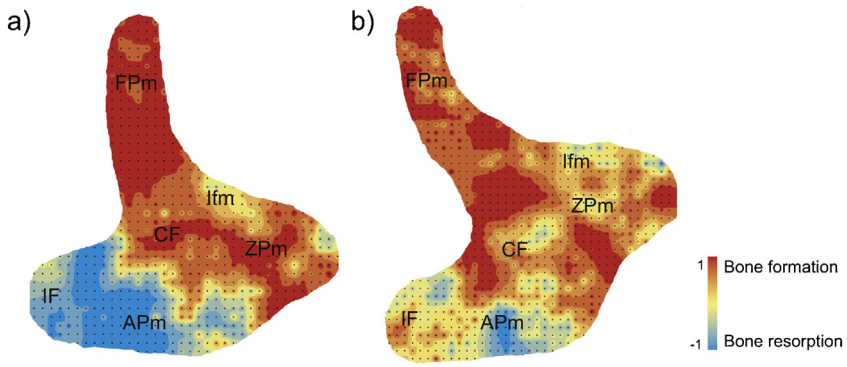

Fig. 6. General bone modeling maps for the subadult (a) and adult (b) maxilla. The points indicate the center of the cells over which the median was calculated. References: FPm, Frontal Process of maxilla; ZPm, Zygomatic Process of maxilla; APm, Alveolar Process of maxilla; CF, Canine Fossa; IF, Incisive Fossa; Ifm, Infraorbital foramen.

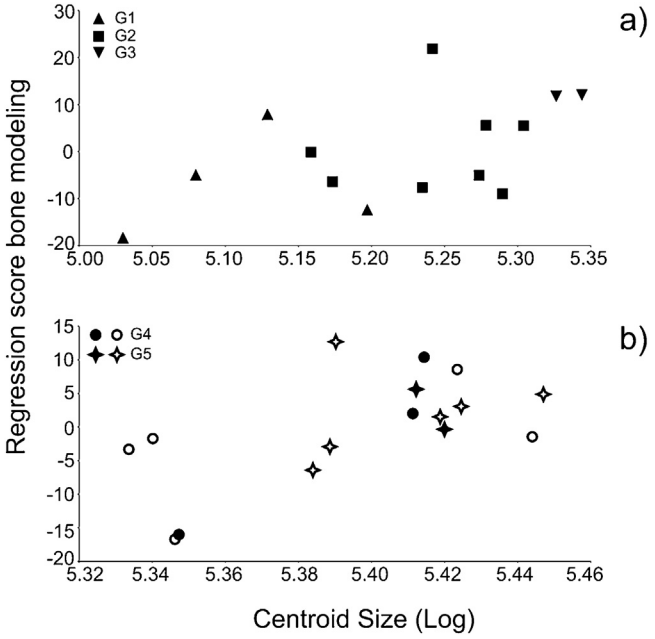

Fig. 7. Regression of bone modeling and centroid size of the maxilla in subadults (a) and adults (b). Subadults: G1, <4.4 years; G2, 4.5–10.4 years; G3, 10.5–14.4 years. Adults: G4, 20–34 years; G5, 35–49 years. Sex of adults is represented as filled (male) and open symbols (female).

Fig. 8 shows the covariation between the shape and bone modeling components of the maxilla in subadults (a) and adults (b). For subadult individuals, the correlation coefficient was 0.74 ($p = 0.45$, Fig. 8a), while for adults the correlation was 0.91 ($p = 0.06$, Fig. 8b). Even though the value obtained for the subadults was not significant, the first two axes of the PLS analysis show a strong association between both blocks. This pattern is more marked in adult individuals. The first axis of the PLS analysis of subadults, which summarizes the main axis of covariation between shape and modeling pattern, shows that those individuals with predominance of formation in the maxilla are located in the negative extreme, while those located in the opposite extreme have a higher proportion of resorption. In the first axis of the shape variables, the shapes in the negative values are characterized by: a frontal process higher and wider in its upper portion, and displaced toward the medial side; a longer but narrower zygomatic process; an alveolar process displaced upwards; and a more rectangular maxillary body (longer and narrower) (Fig. 8a). In adult individuals, the first axis of bone modeling separates the individuals with the highest proportion of formation toward the positive end and those with more resorption toward the negative side. With respect to the changes in shape associated with bone modeling, it is observed that the morphologies at the positive end of the first axis present: a wider frontal process at the base and narrow at the upper part; a wider zygomatic process; the alveolar process displaced upwards and the body of the maxilla displaced toward the lateral (Fig. 8b).

4. Discussion

Overall, the results obtained here indicate changes in the maxillary shape and great variation in the pattern of bone modeling along the ontogenetic trajectory. In comparison with the subadults, the maxilla of the adult individuals presented a straight body and an anterior projection of the bone as well as an important vertical extension and enlargement of the area between zygomatic and alveolar processes. Likewise, the patterns of bone modeling differ between subadults and adults. The general map for the subadult maxilla presented three clearly distinguishable areas: the region of the frontal process, characterized by the predominance of bone formation; the canine fossa and the zygomatic process, with presence of formation and small areas of bone resorption; and the alveolar process characterized by the predominance of resorption. In adults the areas were not clearly differentiated, with the exception of the alveolar process. The presence of anterior resorption was greater in individuals between 10.5–14.4 years, being restricted to the alveolar process in anterior and posterior age groups. In adults, the extension of the areas of resorption was limited, with the presence of formation even in the incisive fossa.

The pattern of shape changes found here agrees with previous studies that analyze ontogenetic samples of modern populations of different geographic origin by using geometric morphometric techniques. Maxillary growth is associated with a greater increase in height than antero-posterior length, a projection of the anterior-inferior maxilla above the incisors and canines, and an increase

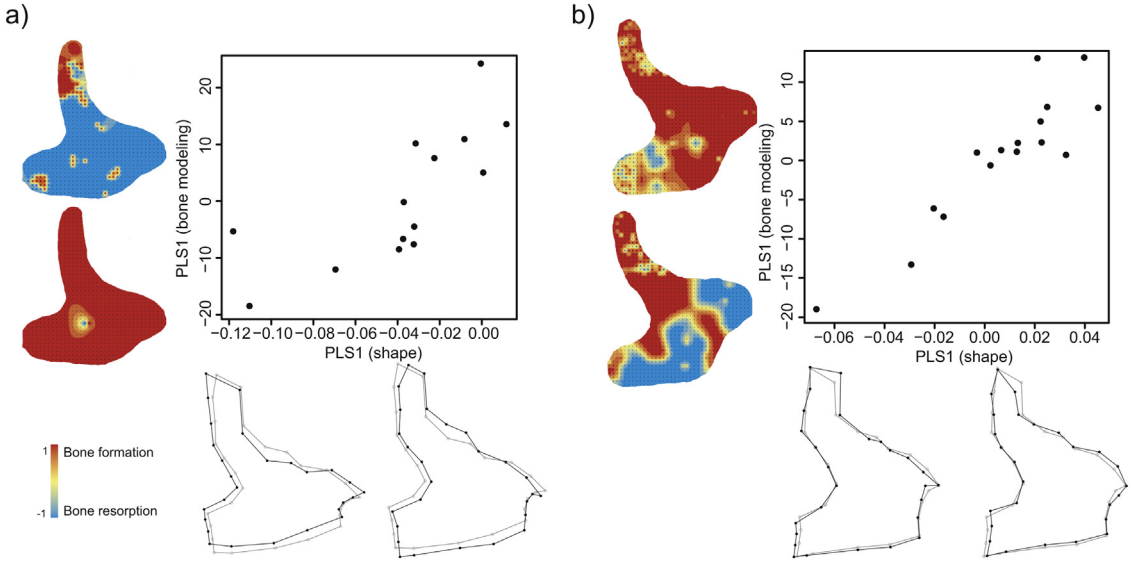

Fig. 8. First axes of the analysis of partial least squares (PLS) between shape and bone modeling of the maxilla in subadults (a) and adults (b).The analyses were made from the coordinates of all landmarks and semilandmarks. To facilitate the visualization of shape changes, only the points on the contour are represented in the wireframe. The gray lines represent the consensus and the black lines represent the shapes at the extremes of the first PLS axis. The bone modeling maps correspond to the extreme individuals along the first PLS axis.

in nasal aperture height (Barbeito-Andrés et al., 2012; Freidline et al., 2017; Gonzalez et al., 2011). This is expected given that the main axis of variation in facial shape with growth are shared by human populations even though some population-specific morphologies observed at early ages are accentuated along postnatal ontogeny (Gonzalez et al., 2011; Viðarsdóttir et al., 2002). The verticalization of the maxilla during growth has been associated to a simultaneous process of primary displacement in the anterior and inferior direction, compensated by a subsequent growth and prolongation (Enlow, 1966; Enlow and Hans, 1996). The continuous bone deposition on the tuberosity would contribute to the horizontal elongation of the dental arch that associated with the presence of resorption in the endosteal surface, generates the space of the maxillary sinus. The presence of anterior resorption would contribute, along with deposition in the frontal process, to the inferior displacement of the arch (Enlow and Bang, 1965; Enlow and Hans, 1996; Kurihara et al., 1980). However, recent studies show that bone modeling patterns are more variable than proposed by these models.

Congruent with the results reported here, the analysis of bone surfaces has shown that unlike other regions of the face, the maxilla displays high levels of variation among individuals in the distribution of formation and resorption activities, particularly in the region of the incisive and canine fossa, and in the zygomatic and alveolar processes. This has been observed especially among subadult individuals (Freidline et al., 2017; Martinez-Maza et al., 2013; McCollum, 2008). Significant changes are also observed during ontogeny, while subadults are characterized by similar extensions of resorptive and formation surfaces, adults exhibit large patches of bone formation (Martinez-Maza et al., 2013; McCollum, 2001, 2008). The alternation of areas with different bone activity in the maxilla could be related to functional demands of mastication. Bone tissues are very responsive to mechanical stimuli, being the period between puberty and young adulthood the most sensitive (Gosman, 2012; Martin et al., 2015), which agree with the interval of maximum variation in the pattern of bone modeling in the sample analyzed here.

The integration of quantitative data of bone modeling and morphology through multivariate statistical analysis has allowed us to evaluate, for the first time, to what extent the morphological variation of the maxilla corresponds to changes in the distribution of the areas of formation and resorption. The results obtained for the covariation between bone modeling and bone morphology indicate that there is no significant association between the variation in size and the distribution of areas of formation and resorption, neither in subadultsnor in adults. This suggests that other mechanisms such as the formation rate could be more relevant to account for changes in maxillary size during ontogeny. Changes in the rate of bone formation can be evaluated, for example, by analyzing the degree of organization of cortical tissue components in histological sections (García Gil et al., 2016; Martinez-Maza, 2007); however, this is difficult to apply in archeological and fossil specimens because it involves the destruction of the samples. In contrast, we found that the changes observed in the shape of the maxilla within each age group, subadults and adults, were associated with changes in the bone modeling patterns. The presence of bone formation was associated with a relatively wider frontal process and a displacement of the alveolar process upwards. This agrees with the expectation of a greater downward displacement of the nasomaxillary complex due to the presence of anterior resorption (Enlow and Bang, 1965; Enlow and Hans, 1996; Martinez-Maza et al., 2013). Conversely, in adults larger areas of bone formation were associated with an inferior projection. This difference between the direction of displacement and the bone modeling could be consequence of a differential contribution of modeling in the region of the tuberosity. In fact, Martinez-Maza (2007) found variation in the modeling pattern of the tuberosity, which was associated to the dental development. However, it is possible that such variation could also contribute to the direction of displacement. Further studies are needed to evaluate to what extent the bone modeling of the tuberosity also affects the projection of the maxillary arch.

In sum, this study contributes to the understanding of the mechanisms and processes that model maxillary morphology during growth. The approach used here allows for the quantitative analysis of various organizational scales which contain information from higher and lower levels in which different mechanisms and processes operate. In this sense, this work contributes to the integration of quantitative data that describe bone modeling and craniofacial morphology. The methodology used to map the relationship between variations in the distribution of the areas of formation-resorption and in the size and shape of the maxilla during ontogeny can easily be extended to other facial structures and to the analysis of the processes underlying the differentiation morphological between sexes, populations, and even species.

Funding

This work was supported by the National Agency for Science and Technology Promotion (PICT 2014-1810, PICT 2014-2134), the National Scientific and Technical Research Council (PIP 0729, PIP 0603) and the National University of La Plata (Subsidio Jóvenes Investigadores 2017).

Acknowledgments

We thank Fabián G. Tricárico (Museo Bernardino Rivadavia) and Diego Gobbo (División Arqueología, Museo de La Plata) for their assistance at different stages of the study; and the staff of the División Antropología (Facultad de Ciencias Naturales y Museo, UNLP) for allowing and facilitating access to the samples.

Appendix A. Supplementary data

Supplementary data associated with this article can be found, in the online version, at https://doi.org/10.1016/j.aanat.2018.10.008.

References

Abdi, H., 2010. Partial least squares regression and projection on latent structure regression (PLS Regression). WIREs Comput. Stat. 2, 97–106.
AlQahtani, S.J., Hector, M.P., Liversidge, H.M., 2010. The London atlas of human tooth development and eruption. Am. J. Phys. Anthropol. 142, 481–490.
Atchley, W.R., Hall, B.K., 1991. A model for development and evolution of complex morphological structures. Biol. Rev. 66, 101–157.
Baffi, E.I., Torres, M.F., Cocilovo, J.A., 1996. La población prehispánica de Las Pirguas (Salta, Argentina). Un enfoque integral. Rev. Arg. Antropol. Biol. 1, 204–218.
Baldini, M.I., Baffi, E.I., Salaberry, M.T., Torres, M.F., 2003. Candelaria: una aproximación desde un conjunto de sitios localizados entre dos cerros de Las Pirguas y el Alto del Rodeo. In: Ortiz, G., Ventura, B. (Eds.), La mitad verde del mundo andino. EFIUNJU, Jujuy, pp. 131–152.
Barbeito-Andrés, J., Pucciarelli, H.M., Sardi, M.L., 2011. An ontogenetic approach to facial variation in three Native American populations. Homo 62, 56–67.
Barbeito-Andrés, J., Sardi, M.L., Anzelmo, M., Pucciarelli, H.M., 2012. Matrices funcionales e integración morfológica. Un estudio ontogénico de la bóveda y el maxilar. Rev. Arg. Antrop. Biol. 14, 79–87.
Bastir, M., 2008. A systems-model for the morphological analysis of integration and modularity in human craniofacial evolution. J. Anthropol. Sci. 86, 37–58.
Bernal, V., Perez, S.I., Gonzalez, P.N., 2006. Variation and causal factors of craniofacial robusticity in Patagonian hunter-gatherers from the late Holocene. Am. J. Hum. Biol. 18, 748–765.
Bookstein, F.L., 1989. "Size and Shape": a comment on semantics. Syst. Zool. 38, 173–180.
Bookstein, F.L., 1991. Morphometric Tools for Landmark Data: Geometry and Biology. Cambridge University Press, Cambridge.
Bookstein, F.L., Sampson, P.D., Streissguth, A.P., Barr, H.M., 1990. Measuring "dose" and "response" with multivariate data using partial least squares techniques. Commun. Stat. Theory 19, 765–804.

Boyde, A., 1972. Scanning electron microscope studies of bone. In: Bourne, G.H. (Ed.), The Biochemistry and Physiology of Bone. Academic Press, New York, pp. 259–310.
Brachetta-Aporta, N., 2016. Error intraobservador en el análisis paleohistológico de superficies craneofaciales. Rev. Arg. Antrop. Biol. 18, 1–9.
Brachetta-Aporta, N., 2018. Dinámica del crecimiento óseo facial en poblaciones humanas del sur de Sudamérica (Ph.D. thesis). Facultad de Ciencias Naturales y Museo, Universidad Nacional de La Plata, Argentina.
Brachetta-Aporta, N., Gobbo, D., 2017. Técnicas de análisis espacial del modelado óseo en superficies craneofaciales. In: XIII Jornadas Nacionales de Antropología Biológica, AABA, Necochea, p129.
Brachetta-Aporta, N., Martinez-Maza, C., Gonzalez, P., Bernal, V., 2014. Bone modeling patterns and morphometric creaniofacial variation in individuals from two prehistoric human populations from Argentina. Anat. Rec. 297, 1829–1838.
Brachetta-Aporta, N., Gonzalez, P.N., Bernal, V., Martinez-Maza, C., 2016. Cambios morfológicos en la mandíbula durante la ontogenia: un aporte desde la histología y la morfometría geométrica. Rev. Arg. Antrop. Biol. 18, 1–11.
Brachetta-Aporta, N., Gonzalez, P., Bernal, V., 2018. A quantitative approach for analysing bone modelling patterns from craniofacial surfaces in hominins. J. Anat. 232, 3–14.
Bromage, T.G., 1984. Interpretation of scanning electron microscopic images of abraded forming bone surfaces. Am. J. Phys. Anthropol. 64, 161–178.
Bromage, T.G., 1989. Ontogeny of the early human face. J. Hum. Evol. 18, 751–773.
Buikstra, J., Ubelaker, D., 1994. Standards for Data Collection from Human Skeletal Remains. Arkansas Archaeological Survey, Fayetteville.
Carnese, F., Mendisco, F., Keyser, C., Dejean, C.B., Dugoujon, J.M., Bravi, C.M., Ludes, B., Crubézy, E., 2010. Paleogenetical study of pre-Columbian samples from Pampa Grande (Salta, Argentina). Am. J. Phys. Anthropol. 141, 452–462.
Cocilovo, J.A., Varela, H.H., 2010. La distribución de la deformación artificial del cráneo en el área Andina Centro Sur. Relaciones 35, 41–68.
Dejean, C.B., Seldes, V., Russo, M.G., Mendisco, F., Keyser, C., Ludes, B., Carnese, F.R., 2014. Variabilidad genética mitocondrial: comparación de muestras de dos sitios arqueológicos del Noroeste argentino. Rev. Arg. Antrop. Biol. 16, 5–16.
Drake, A.G., Klingenberg, C.P., 2008. The pace of morphological change: historical transformation of skull shape in St. Bernard dogs. Proc. R. Soc. Lond. B Biol. Sci. 275, 71–76.
Enlow, D.H., 1966. A comparative study of facial growth in Homo and Macaca. Am. J. Phys. Anthropol. 24, 293–308.
Enlow, D.H., Bang, S., 1965. Growth and remodeling of the human maxilla. Am. J. Orthod. 51, 446–464.
Enlow, D.H., Hans, M.G., 1996. Essentials of Facial Growth. WB Saunders, Philadelphia.
Franz-Odendaal, T.A., 2011. Epigenetics in bone and cartilage development. In: Hallgrímsson, B., Hall, B.K. (Eds.), Epigenetics: Linking Genotype and Phenotype in Development and Evolution. University of California Press, California, pp. 195–220.
Freidline, S.E., Martinez-Maza, C., Gunz, P., Hublin, J.J., 2017. Exploring modern human facial growth at the micro- and macroscopic levels. In: Percival, C.J., Richtsmeier, J.T. (Eds.), Building Bones: Bone Formation and Development in Anthropology. Cambridge University Press, Cambridge, pp. 104–127.
Frost, H.M., 1987. Bone "Mass" and the "Mechanostat": a proposal. Anat. Rec. 219, 1–9.
García Gil, O., Cambra-Moo, O., Audije Gil, J., Nacarino-Meneses, C., Rodríguez Barbero, M.A., Rascón Pérez, J., González Martín, A., 2016. Investigating histomorphological variations in human cranial bones through ontogeny. C. R. Palevol 15, 527–535.
González, A.R., 1972. Descubrimiento arqueológico en la Serranía de Las Pirguas. Pcia. de Salta. Univ. Nac. La Plata 24, 388–392.
Gonzalez, P.N., Perez, S.I., Bernal, V., 2010. Ontogeny of robusticity of craniofacial traits in modern humans: a study of South American populations. Am. J. Phys. Anthropol. 142, 367–379.
Gonzalez, P.N., Perez, S.I., Bernal, V., 2011. Ontogenetic allometry and cranial shape diversification among human populations from South America. Anat. Rec. 294, 1864–1874.
Gosman, J.H., 2012. Growth and development: morphology, mechanisms, and abnormalities. In: Crowder, C., Stout, S. (Eds.), Bone Histology: An Anthropological Perspective. CRC Press, Boca Raton, pp. 23–44.
Gunz, P., Mitteroecker, P., 2013. Semilandmarks: a method for quantifying curves and surfaces. Hystrix 24, 103–109.
Hall, B.K., 2003. Unlocking the black box between genotype and phenotype: cell condensations as morphogenetic (modular) units. Biol. Philos. 18, 219–247.
Hallgrimsson, B., Lieberman, D.E., 2008. Mouse models and the evolutionary developmental biology of the skull. Integr. Comp. Biol. 48, 373–384.
Hammer, Ø., Harper, D.A.T., Ryan, P.D., 2001. PAST: paleontological statistics software package for education and data analysis. Palaeontol. Electronica 4, 1–9.
Klingenberg, C.P., 2011. MorphoJ: an integrated software package for geometric morphometrics. Mol. Ecol. Resour. 11, 353–357.
Klingenberg, C.P., 2013. Visualizations in geometric morphometrics: how to read and how to make graphs showing shape changes. Hystrix 24, 15–24.
Klingenberg, C.P., 2016. Size, shape, and form: concepts of allometry in geometric morphometrics. Dev. Genes Evol. 226, 113–137.
Kurihara, S., Enlow, D.H., Rangel, R.D., 1980. Remodeling reversals in anterior parts of the human mandible and maxilla. Angle Orthod. 50, 98–106.
Lacruz, R.S., Bermúdez de Castro, J.M., Martinón-Torres, M., O'Higgins, P., Paine, M.L., Carbonell, E., Arsuaga, J.L., Bromage, T.G., 2013. Facial morphogenesis of the Earliest Europeans. PLoS One 8, e65199.
Lacruz, R.S., Bromage, T.G., O'Higgins, P., Arsuaga, J.L., Stringer, C., Godinho, R.M., Warshaw, J., Martínez, I., Gracia-Tellez, A., Bermúdez de Castro, J.M., Carbonell, E., 2015a. Ontogeny of the maxilla in Neanderthals and their ancestors. Nat. Commun. 6, 8996.
Lacruz, R.S., Bromage, T.G., O'Higgins, P., Toro-Ibacache, V., Warshaw, J., Berger, L.R., 2015b. Distinct growth of the nasomaxillary complex in Au. Sediba. Sci. Rep. 5, 15175.
Lema, V.S., 2009. Criterios de selección en los procesos de manipulación vegetal: el potencial de la información etnobotánica en la interpretación de restos arqueobotánicos de Cucurbita sp. Darwiniana 47 (1), 35–55.
Lema, V.S., 2011. The possible influence of post-harvest objectives on *Cucurbita maxima* subspecies *maxima* and subspecies *andreana* evolution under cultivation at the Argentinean Northwest: an archaeological example. Archaeol. Anthropol. Sci. 3, 113–139.
Lieberman, D.E., 2011. The Evolution of the Human Head. Harvard University Press, Cambridge.
Maggiano, C.M., 2012. Making the mold: a microstructural perspective on bone modeling during growth and mechanical adaptation. In: Crowder, C., Stout, S. (Eds.), Bone Histology: An Anthropological Perspective. CRC Press, Boca Raton, pp. 45–90.
Martin, B.R., Burr, D.B., Sharkey, N.A., Fyhrie, D.P., 2015. Skeletal Tissue Mechanics. Springer, New York.
Martinez-Maza, C., 2007. Ontogenia y filogenia del modelado óseo en el esqueleto facial y la mandíbula de los hominoideos. Estudio de la línea filogenética neandertal a partir de las muestras de Atapuerca-SH y El Sidrón (Ph.D. thesis). Facultad de Ciencias Biológicas, Universidad Complutense de Madrid, Madrid.
Martinez-Maza, C., Rosas, A., Nieto-Diaz, M., 2010. Identification of bone formation and resorption surfaces by reflected light microscopy. Am. J. Phys. Anthropol. 143, 313–320.
Martinez-Maza, C., Rosas, A., Nieto-Diaz, M., 2013. Postnatal changes in the growth dynamics of the human face revealed from the bone modelling patterns. J. Anat. 223, 228–241.
Martinez-Maza, C., Freidline, S.E., Strauss, A., Nieto-Diaz, M., 2016. Bone growth dynamics of the facial skeleton and mandible in *Gorilla gorilla* and *Pan troglodytes*. Evol. Biol. 43, 63–80.
Martínez-Vargas, J., Muñoz-Muñoz, F., Martinez-Maza, C., Molinero, A., Ventura, J., 2017. Postnatal mandible growth in wild and laboratory mice: differences revealed from bone remodeling patterns and geometric morphometrics. J. Morphol. 278, 1058–1074.
McCollum, M.A., 2001. Variation in the growth and modeling of the human maxilla as revealed by scanning electron microscopy. Scanning 23, 71.
McCollum, M.A., 2008. Nasomaxillary remodeling and facial form in robust Australopithecus: a reassessment. J. Hum. Evol. 54, 2–14.
McCollum, M.A., Ward, S.C., 1997. Subnasoalveolar anatomy and Hominoid phylogeny: evidence from comparative ontogeny. Am. J. Phys. Anthropol. 102, 377–405.
Meindl, R.S., Lovejoy, C.O., 1985. Ectocranial suture closure: a revised method for the determination of skeletal age at death based on the lateral-anterior sutures. Am. J. Phys. Anthropol. 68, 57–66.
Menéndez, L., Bernal, V., Novellino, P., Perez, S.I., 2014. Effect of bite force and diet composition on craniofacial diversification of southern South American human populations. Am. J. Phys. Anthropol. 155, 114–127.
Mitteroecker, P., Bookstein, F., 2008. The evolutionary role of modularity and integration in the hominoid cranium. Evolution 62, 943–958.
Mitteroecker, P., Gunz, P., 2009. Advances in geometric morphometrics. Evol. Biol. 36, 235–247.
Monteiro, L.R., 1999. Multivariate regression models and geometric morphometrics: the search for causal factors in the analysis of shape. Syst. Biol. 48, 192–199.
Moss, M.L., Young, R.W., 1960. A functional approach to craniology. Am. J. Phys. Anthropol. 18, 281–292.
O'Higgins, P., Jones, N., 1998. Facial growth in *Cercocebus torquatus*: an application of three-dimensional geometric morphometric techniques to the study of morphological variation. J. Anat. 193, 251–272.
O'Higgins, P., Bromage, T.G., Johnson, D.R., Moore, W.J., McPhie, P., 1991. A study of facial growth in the sooty mangabey *Cercocebus atys*. Folia Primatol. 56, 86–94.
R Core Team, 2014. R: a language and environment for statistical computing. R Foundation for Statistical Computing, Vienna, Austria, URL https://www.R-project.org/.
Rohlf, F.J., 2015. The tps series of software. Hystrix 26, 9–12.
Rohlf, F.J., Corti, M., 2000. Use of two-block partial least-squares to study covariation in shape. Syst. Biol. 49, 740–753.
Rohlf, F.J., Slice, D.E., 1990. Extensions of the Procrustes method for the optimal superimposition of landmarks. Syst. Zool. 39, 40–59.
van Buuren, S., Groothuis-Oudshoorn, K., 2011. mice: Multivariate Imputation by Chained Equations in R. J. Stat. Softw. 45, 1–67.
Viðarsdóttir, U.S., O'Higgins, P., Stringer, C., 2002. A geometric morphometric study of regional differences in the ontogeny of the modern human facial skeleton. J. Anat. 201, 211–229.
von Arx, T., Lozanoff, S., 2017. Clinical Oral Anatomy: A Comprehensive Review for Dental Practitioners and Researchers. Springer International Publishing, Switzerland.
Wealthall, R.J., 2002. Surface remodelling of the facial skeleton in juvenile *Macaca mulatta*: implications for sexual dimorphism. Folia Primatol. 73, 49–53.